

Development of a Galfenol Magnetostrictive Linear Motor with Low Driving Voltage

Ran Zhao

Jiangxi Province Key Laboratory of Precision Drive & Control, Nanchang Institute of Technology, China, Tianxiang Road No.289 High and New Technology Industrial Development Zone of Nanchang City, (zhaoran@nit.edu.cn)

Abstract

A Galfenol driven miniature linear motor was developed in this paper. The proposed motor realized the micro stepping motion and based on the inertia impact and friction force. At first, the principle of impact driving mechanism was introduced, with the discussion of the structure of the given motor. Then, the analysis of the motor's impedance property and shaft displacement was presented by simulations. At last, the performance of the proposed motor was tested by experiments. The experimental results demonstrate that the micro motor is capable of 8 nm resolution over the travel range of 30 mm. The maximum step-size is 2.1 μm . The maximum operation frequency is 500 Hz. A high accuracy displacement was achieved under 0-3 V low driving voltage. The results imply that the given motor is highly promising for use in nano-scale positioning system.

Key words

Galfenol, Magnetostrictive material, Precision positioning, Inertia impact

1. Introduction

In recent years, the demand for precision positioning devices is increasing. Various precision motors, including inchworm motor, inertial impact motor and ultrasonic motor, have been widely used in the fields of optics, semiconductors, bio-medicine and robotic industry. To achieve nano scale displacement control, people began to use intelligent materials as motor-driven elements

instead of traditional electromagnetic motors. Since its invention, piezoelectric motor has been implemented in industrial applications [1].

Piezoelectric motors have the advantages of simple structure, easy operation, and low manufacturing cost. But there are still some disadvantages, the high driving voltage (30-150 V), short service life (1-2 years) and the impedance matching problem of the power supply [2-5]. These shortcomings have prompted scholars to find new functional materials such as replacing piezoelectric material in magnetostrictive materials (Terfenol-D). Terfenol-D is applied due to its characteristics of large magnetostriction in room temperature, fast response and long service life. J. Kim developed a three-phase excitation magnetostrictive linear motor [6,7], whose working frequency is about 10 Hz. B. T. Yang designed a self-moving magnetostrictive inchworm linear motor [8], whose working frequency is 25 Hz. Q. G. Lu & R. Zhao developed an impact type magnetostrictive motor [9], and its working frequency is 100 Hz with velocity of 250 $\mu\text{m/s}$.

However, due to the high saturation magnetic field of Terfenol-D (400-600 kA/m) [10], the magnetostrictive motors usually have a huge volume. Meanwhile, the hysteresis effect caused by the excitation coil limits its working frequency. Galfenol (Fe-Ga alloy) is a new kind of magnetostrictive material appearing after Terfenol-D. It has low saturation magnetic field (9-20 kA/m) and excellent mechanical properties [11], which makes it applied to micro&nano devices. According to current study, the magnetostriction coefficient of Galfenol has reached 200-400 ppm. Its strain coefficient is half of PZT (400-800 ppm), and saturation magnetic field is only 1/20 of Terfenol-D. The application of Galfenol as drive element will reduce the turns of the driving coil, and make the actuator more compact. Meanwhile, it increases motor's working frequency and displacement resolution.

Based on this, a novel magnetostrictive material, Galfenol, is used as the driving element for linear motor in order to reduce the current loss, miniaturize the size and improve the motion performance of the motor. The aim of this research is to develop a miniature, low voltage driven and high resolution linear motor. In section two, the design and operation principle are discussed. Then the dynamic model of the motor is established in section three. With this model, the motor's output step-size can be predicted. At last, to investigate the performance of the given motor, we establish an experimental system, and test the maximum operation frequency and the minimum step-size of the motor.

2. Operation Principle

Typical impact drive mechanisms (IDM) rely on the inertial impact and friction force to achieve movement [12]. Firstly, by utilizing the asymmetry of the saw-tooth signal, the driving element will generate the inertial impact force during the elongation or contraction process. Then, under the acts of the inertia and the friction force, the step movement can be achieved. Fig. 1(a) shows the actuator fixed type IDM's structure. The magnetostrictive actuator is fixed to the base, and the drive element (Galfenol rod) inside is directly connected to the shaft. The movable part of the motor is the slider. The typical inertial impact movement process can be divided into three periods:

(1) In Stage 1, the initial period, there is no input current applied to the magnetostrictive actuator. The Galfenol rod remains at its initial length, and the motor at the initial position.

(2) In Stage 2, the extension period, the Galfenol rod slowly expands as the input current is slowly increased. During this period, the slider moves with the motor shaft. If the friction force between the slider and the shaft is large enough to overcome the inertial force generated by the magnetostrictive actuator, there is no relative movement.

(3) In Stage 3, the retraction period, the Galfenol rod quickly contract back in a very short time when the input current rapidly decreases. In this period, the friction force between the main object and the ground is not sufficiently large to overcome the inertial force of the mass block. Therefore, the sliding part will slip over a distance.

(4) The reverse motion can be realized by changing the order of extension and retraction process.

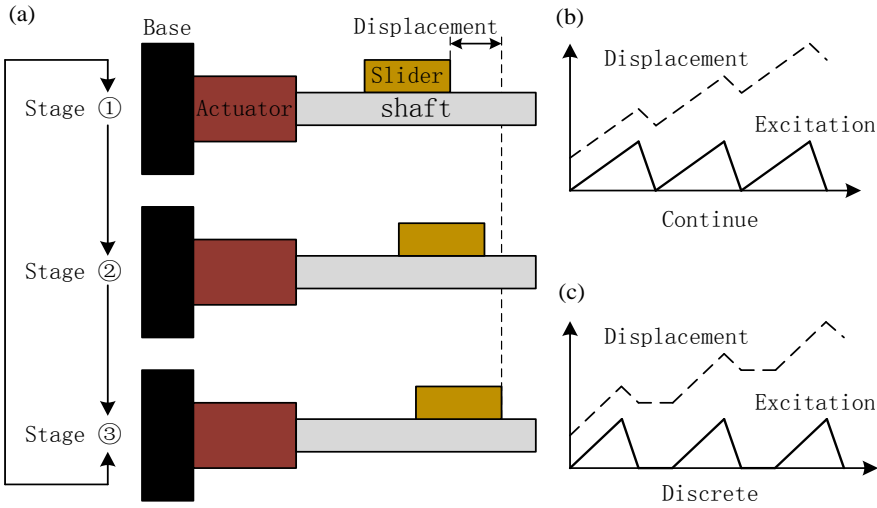


Fig.1. Principle of the IDM

According to the discussion from Reference [13], there are two main methods to drive the inertial impact mechanism-continuous and discrete driving strategies (See Fig. 1(b) and Fig. 1(c)). When using continuous saw-tooth signal, the motor operates in the "slip" mode with the movement trajectory close to line. When the discrete saw-tooth signal is taken, the motor operates in the "stick" mode, generating a typical stepped motion. The continuous drive strategy is simpler, but will cause the loss of step-size. The discrete driving strategy can obtain high precision output step-size, and improve the motor's efficiency.

3. Design

3.1 Structure

Fig.2 (a) displays the photograph of Galfenol motor. Its oversize is $\Phi 24 \text{ mm} \times 85 \text{ mm}$. The slider's size is $12 \text{ mm} \times 12 \text{ mm} \times 16 \text{ mm}$. The designed positioning distance 30 mm . The motor is fixed by the holder to prevent vibration. Fig.2 (b) shows the structure of the given motor, which includes the Galfenol rod, bobbin, coil, housing, preload spring, shaft, linear bearing and slider. The preload spring can make the Galfenol rod and the shaft face closely fit, which is good for the transfer of the force and displacement. Furthermore, it can provide a prestress to the magnetostrictive rod, to increase the saturation magnetostriction. A linear bearing is used to fix and guide the direction of movement of the motor shaft, while reducing the resistance to axial movement.

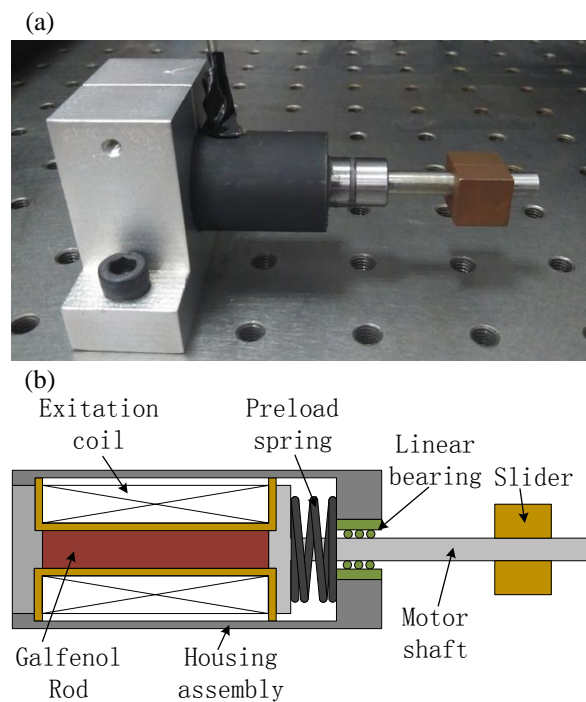


Fig.2. The Magnetostrictive IDM (a) Photo of the motor (b) Schematic of the motor

3.2 Magnetostrictive Material

Table.1 shows the parameters of Galfenol rod used in this paper. Its saturation magnetostrictive coefficient is 260 ppm. But taking into account the effect of the preloaded spring, the magnetostrictive rod withstands under a certain pressure of about 10 MPa. So we tested the Galfenol rod's magnetostrictive coefficient under 10 MPa circumstance. The experimental λ - H curve is displayed in Fig.3. Under this condition, the saturation magnetic field is 15 kA/m, and the saturation magnetostrictive coefficient 306 ppm. In order to improve the output linearity of the motor, the near-linear region (2-10 kA/m) can be selected as the excitation magnetic field. To get a larger output step-size, the saturation magnetic field strength of 15 kA/m can also be chosen as the upper limit of the excitation magnetic field. At this time, the Galfenol rod's magnetostriction is 10.71 μm .

Table.1 The Parameters of Galfenol rod

Name	Value	Unit
Young's modulus	120	GPa/m2
Saturation magnetostrictive coefficient	260	ppm
Saturation magnetic field	12	kA/m
Curie temperature	535	$^{\circ}\text{C}$
Diameter	8	mm
Length	35	mm

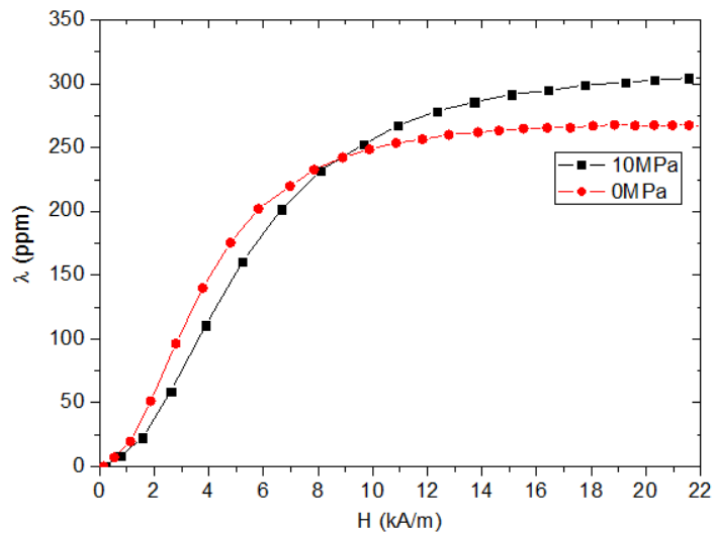


Fig.3. The Magnetostriction of Galfenol rod

The magnetostrictive coefficient can be calculated by the second order domain rotation equation [14],

$$\lambda = \frac{3\lambda_s}{2M_s^2} M^2 \quad (1)$$

where λ is the saturation magnetostriction, λ_s is the saturation magnetostriction coefficient; M is the magnetization, M_s is the saturation magnetization.

3.3 Magnetic field

To calculate the magnetic field, two assumptions should be claimed as follows: (1) zero leakage flux and (2) no air gap in the magnetic field. A similar ideal model and its analysis are given in reference [15]. By employing Ampere's Circuital Law, the magnetic field can be expressed as,

$$H = \oint_i nIdl = \frac{N}{l_r} I \quad (2)$$

where n is the turns per unit length, N is the total turns of the coil, l_r is the length of Galfenol rod, I is the excitation current. When the excitation current is limited to 2 A, the total turns of the coil can be calculated by Eq. (3),

$$N = \frac{H_s l_r}{I_s} \quad (3)$$

where H_s is the saturation field and I_s is the saturation current. When $H_s=15$ kA/m, $I_s=2$ A, $l_r=0.035$ m, the calculated value of the coil's total amount of turns is 262.5. Meanwhile, we make $N=260$ in reality.

4. Simulation and Analysis

4.1 Impedance Analysis

The circuit parameters of the proposed motor are tested by a LCR bridge. The RL series impedance model is used to represent the driving coil (see Fig.4 (a)). The equivalent inductance L is 272 μ H, and the equivalent resistance $R=740$ m Ω . With these parameters, the impedance frequency characteristic curves can be simulated by Matlab software. Fig.4 (b) shows the simulation results. The given motor has a high resonant frequency, meaning the motor can work at a high driving frequency without considering the thermal loss effect of coil impedance.

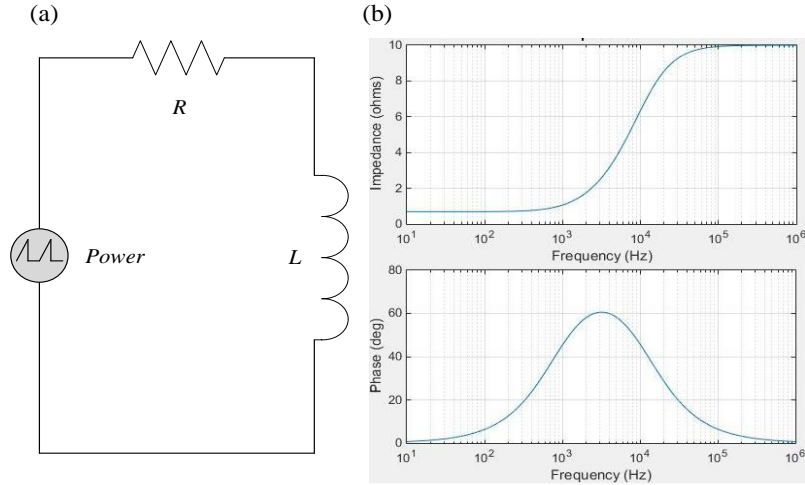


Fig.4. The Impedance of motor (a) Impedance model (b) Impedance characteristics

According to Ohm's Law, the driving voltage can be expressed as follow,

$$V = |Z|I_s = \sqrt{R^2 + (\omega L)^2} I_s \quad (4)$$

By using Eq. (4), when setting the driving frequency $f=1$ kHz, the calculation value of driving voltage is only 3.002 V. This result indicates that the Galfenol motor can work under very low voltage compared to piezoelectric motors.

4.2 FE analysis

In this section, the performance of the proposed motor has been analyzed by using finite element method. The software COMSOL is employed to simulate the displacement of the motor shaft. In this simulation, Eq. (1) is utilized to calculate the magnetostriction of Galfenol rod. The saturation magnetostriction coefficient λ_s is 306 ppm, with the saturation magnetization $\mu_0 M_s=1.6$ T. Fig.5 shows the result, when the excitation current is 2 A, the maximum displacement of the motor shaft is 10.878 μm .

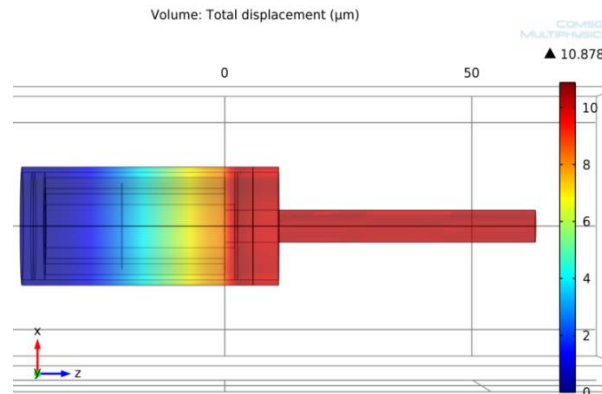


Fig.5. Displacement of motor shaft by FE simulation

5. Experiments and Discuss

5.1 Experimental system

An experimental system has been built to test the performance of the Galfenol motor (see Fig.6). In this experiment, the driving signal was constituted by using dSPACE-ds1103 to generate driving signal and acquire data from measurement instruments. The 0-1 V saw-tooth signal generated by dSPACE was amplified into 0-2 A current by AE7224. A laser displacement sensor Ltc-025 and a grating displacement sensor MTI-2100 were used to measure the displacement and minimum step-size of the Galfenol motor, respectively. All of the analog signals produced by the measuring instruments were collected by dSPACE-ds1103, and then converted to digital signals through its 12-bit AD converter.

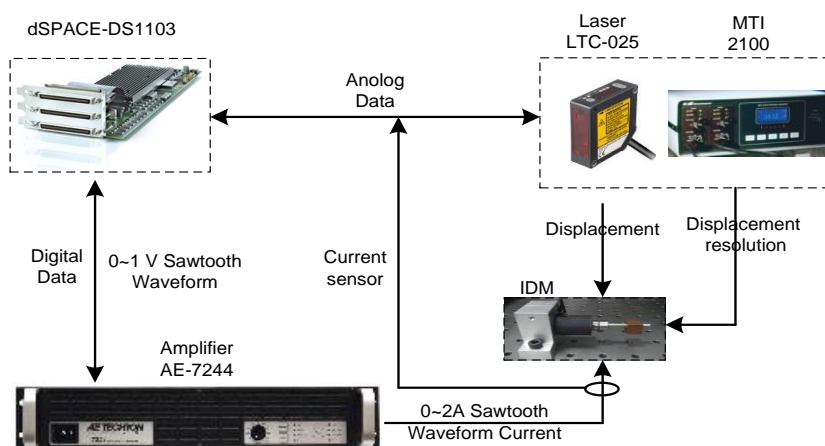


Fig.6. The framework of experimental system

5.2 Experimental Results and Discuss

Fig.7 shows the motion characters of Galfenol driven linear motor. We used discrete saw-tooth signal to drive the motor, as discussed in reference [13], and the motor will output a “step” shape movement trajectory. Fig.7 (a) shows the motor’s displacement when the driving current I is 0.5 A, and the operation frequency is 30 Hz. The given motor works at a low excitation voltage, and outputs a clearly step type motion. The step-size is 0.2 μm .

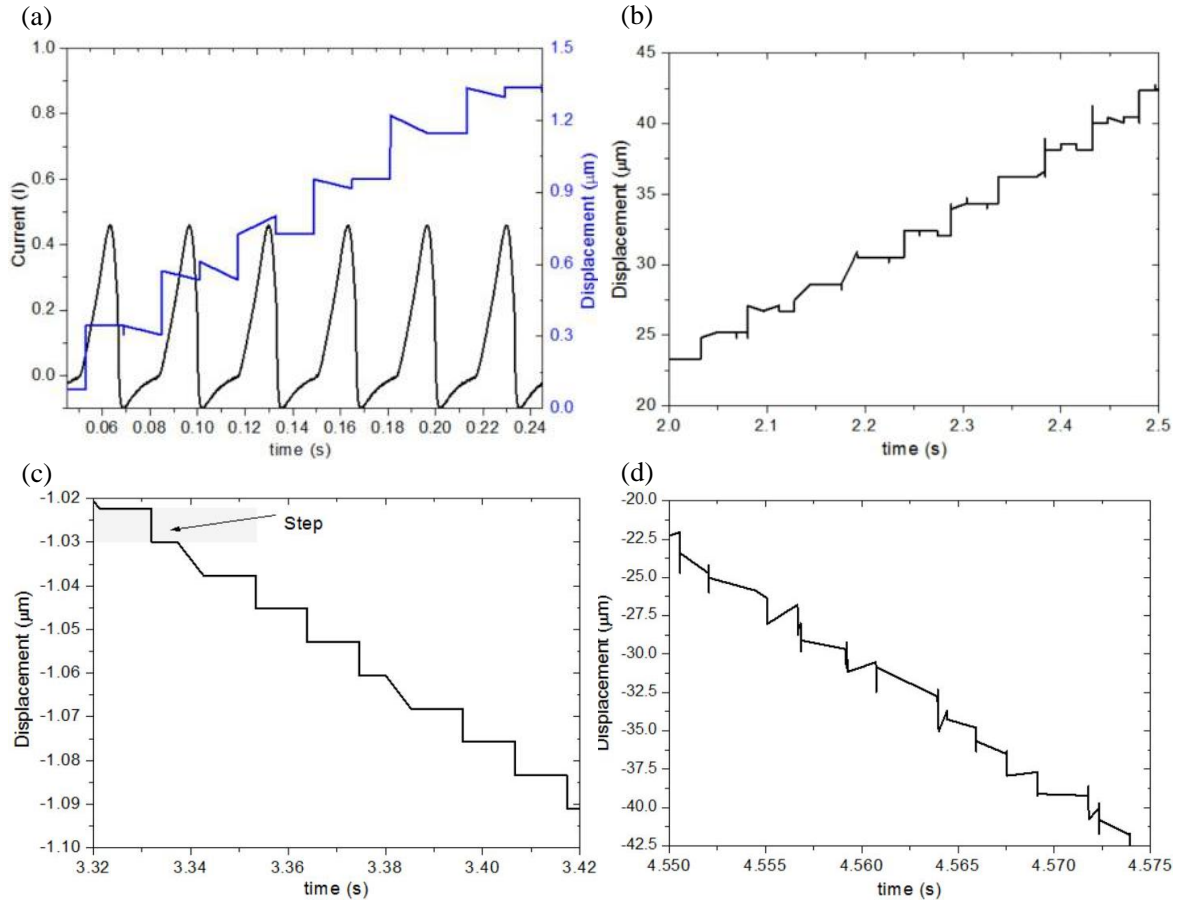


Fig.7. Displacement performance of the Galfenol linear motor

Fig.7 (b) shows that when the driving current increases to 2.0 A, the motor will output a maximum step-size, which is 2.1 μm . The minimum step-size is 8 nm (see Fig.7 (c)), which indicates that the given motor has a very high resolution of displacement. The maximum operation frequency is 500 Hz (see Fig.7 (d)). At this frequency, the Galfenol motor will operate in the “slip-slip” mode, and its motion trajectory is close to a straight line. There are two primary factors limiting the motor’s operation frequency: one is the heat losses induced by the coil, which makes increased temperature of Galfenol rod, thus reducing its magnetostrictive properties; The other one is the hysteresis effect of magnetostrictive material and the process of contraction. The driving element is affected by the hysteresis effect, and cannot be reset immediately.

6. Conclusion

In this study, a Galfenol driven linear step motor was designed and tested. Then we analyzed the impedance and displacement of the motor by simulation. In order to test the performance of the motor, an experimental system was set up to test the motor’s operating frequency and step-size. Finally, through the experiment, it was verified that the Galfenol driven linear motor

can exert excellent motion performance, and its optimized structure will make it more practical. The mainly advantages of the given motor are as follows:

- (1) Low drive voltage, 0-3 V.
- (2) High operation frequency in non-resonant mode, 500 Hz.
- (3) High step resolution, 8 nm.
- (4) Small size, $\Phi 24$ mm \times 85 mm.

Acknowledgments

This work is supported by Opening fund of Jiangxi Province of Jiangxi Province Key Laboratory of Precision Drive & Control under granted No.KFKT201617, University Science and Technology Project under granted No.KJLD14094 and Jiangxi Province Science and Technology Support Program under granted No.20122BBE500033.

References

1. K. Spanner, B. Koc, Piezoelectric Motors, an Overview, 2016, *Actuators*, vol.5, no.1, pp.1-18.
2. T. Morita, T. Nishimura, R. Yoshida, H. Hosaka, Design for the resonant type SIDM (Smooth Impact Drive Mechanism) actuator. 2012, *Proc. Symp. on Ultrason. Electron.* vol.33, pp.77-78.
3. K. Furutani, T. Higuchi, Y. Yamagata, N. Mohri, Effect of lubrication on impact drive mechanism, 1998, *Precis. Eng.*, vol.22, no.2, pp.78–86.
4. N. Henmi, Y. Sumi, M. Tanaka, Fast drive of displacement magnification mechanism with flexure hinge using loading type impact damper, 2010, *J. Mech. Sci. and Tech.*, 2010, vol.24, no.1, pp.211-214.
5. C.F Yang, S.L Jeng, W.H Chieng, Motion behavior of triangular waveform excitation input in an operating impact drive mechanism, 2011, *Sens. Actuators A*, vol.166, pp.66-77.
6. W. Kim, A. Sadighi, A Novel Low-Power Linear Magnetostrictive Actuator With Local Three-Phase Excitation, 2010, *IEEE Trans. Mechatronics*, vol.15, no.2, pp.299-307.
7. A. Sadighi, W. Kim, Sensorless Control of a Novel Linear Magnetostrictive Motor, 2010, *IEEE Trans. Ind. Appl.*, vol.47, no.2, pp.736-743.
8. J. Kim, J. Doo, Magnetostrictive self-moving cell linear motor, 2003, *Mechatronics*, vol.13, no.7, pp.739-753.
9. Q. Lu, R. Zhao, Z. Zhu, Magnetostrictive Lineal Actuator Based on Impact Drive Mechanism. 2015, *Chin. J. Small Spec. Elec. Mach.*, vol.43, pp.9-11.

10. G. Engdahl, Handbook of Giant Magnetostrictive Materials, 1999, Academic Press, New York.
11. J. Atulasimha, A.B Flatau, A review of magnetostrictive iron–gallium alloys, 2011, Smart Materials and Structures, vol.20, pp.1-15.
12. Z.Z Guang, T. Ueno, T. Higuchi, Magnetostrictive Actuating Device Utilizing Impact Forces Coupled with Friction Forces, 2010, IEEE Int. Symp. Ind. Electron., pp.464-469.
13. M. Hunstig, T. Hemsel, W. Sextro, Mechatronics Stick–slip and slip–slip operation of piezoelectric inertia drives. Part I: Ideal excitation, 2013, Sens. Actuators A, vol.200, pp.90-100.
14. D.C Jiles, Introduction to Magnetism and Magnetic Materials, Chapman and Hall, New York, 1991.
15. S. Karunanidhia, M. Singaperumal. Design, analysis and simulation of magnetostrictive actuator and its application to high dynamic servo valve, 2010, Sens. Actuators A, vol.157, pp.185-197.